# Amplification of superkicks in black-hole binaries through orbital eccentricity

Ulrich Sperhake,[1,2,3,*] Roxana Rosca-Mead,[1,†] Davide Gerosa,[4,‡] and Emanuele Berti[5,2,§]

[1]*Department of Applied Mathematics and Theoretical Physics, Centre for Mathematical Sciences, University of Cambridge, Wilberforce Road, Cambridge CB3 0WA, United Kingdom*
[2]*Department of Physics and Astronomy, The University of Mississippi University, Mississippi 38677, USA*
[3]*California Institute of Technology, Pasadena, California 91125, USA*
[4]*School of Physics and Astronomy and Institute for Gravitational Wave Astronomy, University of Birmingham, Birmingham B15 2TT, United Kingdom*
[5]*Department of Physics and Astronomy, Johns Hopkins University, 3400 N. Charles Street, Baltimore, Maryland 21218, USA*

(Received 3 October 2019; published 22 January 2020)

We present new numerical-relativity simulations of eccentric merging black holes with initially antiparallel spins lying in the orbital plane (the so-called *superkick* configuration). Binary eccentricity boosts the recoil of the merger remnant by up to 25%. The increase in the energy flux is much more modest, and therefore this kick enhancement is mainly due to asymmetry in the binary dynamics. Our findings might have important consequences for the retention of stellar-mass black holes in star clusters and supermassive black holes in galactic hosts.

DOI: 10.1103/PhysRevD.101.024044

## I. INTRODUCTION

According to Einstein's theory of general relativity, gravitational waves carry energy, angular momentum, and linear momentum. In a binary black-hole (BH) system, the emission of energy and angular momentum causes the orbit to shrink, eventually leading to the merger of the two BHs. The emission of linear momentum imparts a recoil (or *kick*) to the merger remnant [1–3].

Calculations based on post-Newtonian (PN) theory found BH recoil speeds[1] of $\mathcal{O}(100)$ km/s [4–6]. Numerical-relativity (NR) simulations, however, show that BH recoils can be more than an order of magnitude larger. This is because the vast majority of the linear momentum is emitted during the last few orbits and merger, where spin interactions are particularly prominent and analytic descriptions within the PN framework become inaccurate. In particular, in 2007, several groups realized that binary BHs with spins lying in the orbital plane and antiparallel to each other might receive *superkicks* as large as approximately 3500 km/s [7–9]. Subsequent studies found that even larger kicks, up to approximately 5000 km/s, can be reached by further fine-tuning the spin directions [10–13]. Large kicks strongly affect the dominant mode of gravitational waveforms [14–16], and therefore it should be possible to directly measure their effect with future gravitational wave (GW) observations [17,18]. Further studies targeted hyperbolic encounters [19] and ultrarelativistic collisions (which are not expected to occur in astrophysical settings) [20], where kicks can reach $10^4$ km/s. We refer to Refs. [21–23] for more extensive reviews on the phenomenology of BH recoils.

The occurrence of superkicks has striking astrophysical consequences for both stellar-mass and supermassive BHs. In particular, BH recoils predicted by NR simulations should be compared to the escape speeds of typical astrophysical environments [24].

The stellar-mass BH binaries observed by LIGO and Virgo may form dynamically in globular clusters [25], which present escape velocities in the range 10–50 km/s. These values are smaller even than typical recoil velocities of nonspinning BH binaries [26], which implies that a large fraction of stellar-mass BHs merging in those environments is likely to be ejected [27] (see Ref. [28] for a complementary study on intermediate-mass BHs in globular clusters). This may not be the case for environments with larger escape speeds such as nuclear star clusters [29] or accretion disks in active galactic nuclei [30,31], which might therefore retain a majority of their merger remnants. If able to pair again, the BHs in such an environment can form "second generation" GW events detectable by LIGO and Virgo [32].

*u.sperhake@damtp.cam.ac.uk
†rr417@cam.ac.uk
‡d.gerosa@bham.ac.uk
§berti@jhu.edu

[1]Speeds are dimensionless in natural units ($c = G = 1$). Therefore, the recoil imparted to a BH does not depend on the total mass of the system.

 

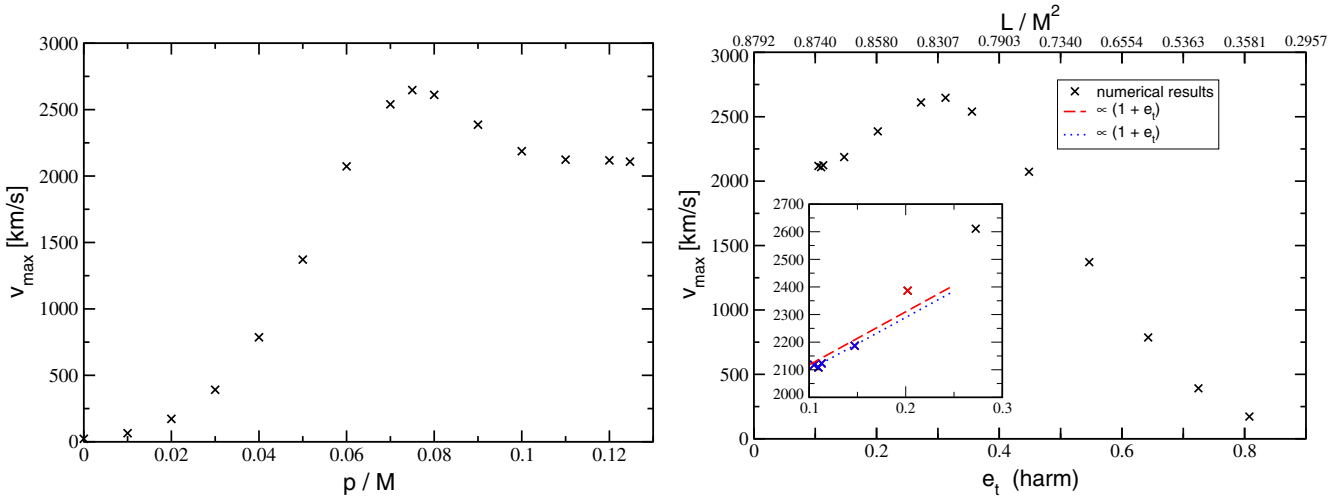


FIG. 1. Superkicks for eccentric binary BHs with equal masses and spins of magnitude $\chi_1 = \chi_2 = 0.596 \simeq 0.6$. *Left*: The maximum kick velocity $v_{\rm max}$ as a function of the linear momentum parameter. The largest kicks correspond to moderate eccentricity and exceed the quasicircular value by about 25%. *Right*: The maximum kick velocity $v_{\rm max}$ as a function of the eccentricity parameter $e_t$ estimated in harmonic gauge. Labels on the upper horizontal axis display the corresponding initial orbital angular momentum $L/M^2$ of the binaries. The inset zooms in on the low-eccentricity regime and shows linear fits $v_{\rm kick} \propto (1 + e_t)$ obtained from the first four, blue data points (dotted curve), and also including the fifth, red data point (dashed curve). The increase of the recoil for small eccentricity is compatible with the $(1 + e)$ scaling from close-limit calculations [44].

The supermassive BH mergers targeted by LISA and pulsar-timing arrays (PTAs) may also be significantly affected by large recoils. Superkicks of $\mathcal{O}(1000)$ km/s exceed the escape speed of even the most massive elliptical galaxies in our Universe. If supermassive BHs are efficiently ejected from their galactic hosts, this decreases their occupation fraction [33] and, consequently, LISA event rates [34,35]. Spin-alignment processes of both astrophysical [36–39] and relativistic [40,41] nature are commonly invoked to mitigate this effect.

Recoils are driven by asymmetries in the merging binary [42,43]; no kick can be imparted if the emission of gravitational wave energy is isotropic. For instance, an equal-mass nonspinning binary does not recoil by symmetry. Unequal masses or misaligned spins, however, introduce asymmetries in the GW emission. Orbital eccentricity is a further natural ingredient to enhance the asymmetry of the binary and, consequently, the kick. Early PN estimates show that, for low eccentricities $e \lesssim 0.1$, the kick imparted to nonspinning BHs increases by about 10%, with a scaling proportional to $1 + e$ [44].

In this paper, we investigate for the first time how superkicks are affected by binary eccentricity using NR simulations of the merger. For this purpose, we consider equal-mass binaries with $M_1 = M_2 \equiv M/2$ with BH spins of equal magnitude pointing in opposite directions inside the orbital plane, $\boldsymbol{S}_1 = -\boldsymbol{S}_2$. Fixing the dimensionless spin $\chi_i \equiv |\boldsymbol{S}_i|/M_i^2$ to $\chi_1 = \chi_2 = 0.596$, we generate a sequence of increasing eccentricity by gradually reducing the initial orbital angular momentum $L$ at fixed binding energy from the quasicircular value to the head-on limit $L = 0$; in practice, we vary for this purpose the initial tangential momentum parameter $p$ of each BH. For a given eccentricity (i.e., fixed $L$), the kick is known to depend sinusoidally on the initial angle of the two spins relative to the line connecting the BHs [14,45,46]. The maximum value of this sine function is the kick reported in Fig. 1 as a function of the linear momentum and of the eccentricity. The significant increase of the maximum kick from about 2100 km/s for approximately quasicircular binaries to 2600 km/s for moderate eccentricities $e_t \sim 0.3$ is the main finding of our study (where $e_t$ is the eccentricity parameter of Ref. [47,48]). We furthermore show that such an increase holds over a wider range of spin magnitudes and correspondingly raises the maximum superkick in BH binaries to about 4200 km/s, larger than the maximum of approximately 3700 km/s for negligible eccentricity.

The rest of this paper presents our methodology and results in more detail and is organized as follows. In Sec. II, we describe our NR runs; in Sec. III, we present our recoil analysis; and in Sec. IV, we discuss the astrophysical relevance of our findings and possible directions for future work.

## II. COMPUTATIONAL FRAMEWORK AND SET OF SIMULATIONS

### A. Numerical-relativity setup

The BH binary simulations reported in this work have been performed with the LEAN code [49], which is based on the CACTUS computational toolkit [50,51]. The Einstein equations are implemented in the form of the Baumgarte-Shapiro-Shibata-Nakamura-Oohara-Kojima formulation

TABLE I. Each sequence of simulations is characterized by the linear momentum parameter $p$ and the initial BH separation $D$ (which determine the orbital angular momentum $L$ and the eccentricity of the binary), as well as the initial spins, given here in both the form of the pristine Bowen-York parameters $\chi_{\mathrm{BY},i}$ and of the more accurate horizon estimate $\chi_i$. The remaining columns list: estimates of the eccentricity $e_t$ obtained from PN relations in the ADMTT and harmonic gauge, respectively; the mean radiated GW energy $E_0$; the maximum kick velocity $v_{\mathrm{max}}$; and the mean spin $\chi_0$ of the remnant BH.

| $p/M$ | $D/M$ | $L/M^2$ | $\chi_{\mathrm{BY},1}=\chi_{\mathrm{BY},2}$ | $\chi_1=\chi_2$ | $e_t$ (ADMTT) | $e_t$ (harm) | $10^2E_0/M$ | $v_{\mathrm{max}}$(km/s) | $\chi_0$ |
|---|---|---|---|---|---|---|---|---|---|
| 0.1247 | 7.000 | 0.8729 | 0.6 | 0.596 | 0.1095 | 0.1096 | 3.687 | 2108 | 0.6815 |
| 0.12 | 7.278 | 0.8734 | 0.6 | 0.596 | 0.1049 | 0.1052 | 3.678 | 2118 | 0.6810 |
| 0.11 | 7.932 | 0.8725 | 0.6 | 0.596 | 0.1130 | 0.1130 | 3.664 | 2123 | 0.6798 |
| 0.10 | 8.678 | 0.8678 | 0.6 | 0.596 | 0.1480 | 0.1472 | 3.757 | 2187 | 0.6808 |
| 0.09 | 9.529 | 0.8576 | 0.6 | 0.596 | 0.2040 | 0.2020 | 3.862 | 2387 | 0.6884 |
| 0.08 | 10.493 | 0.8394 | 0.6 | 0.596 | 0.2758 | 0.2725 | 3.656 | 2611 | 0.6999 |
| 0.075 | 11.018 | 0.8264 | 0.6 | 0.596 | 0.3166 | 0.3124 | 3.368 | 2647 | 0.7010 |
| 0.07 | 11.571 | 0.8100 | 0.6 | 0.596 | 0.3608 | 0.3555 | 3.069 | 2540 | 0.7021 |
| 0.06 | 12.754 | 0.7652 | 0.6 | 0.596 | 0.4567 | 0.4485 | 2.258 | 2073 | 0.6905 |
| 0.05 | 14.013 | 0.7007 | 0.6 | 0.596 | 0.5603 | 0.5467 | 1.452 | 1371 | 0.6539 |
| 0.04 | 15.288 | 0.6115 | 0.6 | 0.596 | 0.6681 | 0.6428 | 0.833 | 786 | 0.5862 |
| 0.03 | 16.487 | 0.4946 | 0.6 | 0.596 | 0.7835 | 0.7247 | 0.429 | 391 | 0.4839 |
| 0.02 | 17.488 | 0.3498 | 0.6 | 0.596 | 1.0122 | 0.8078 | 0.203 | 172 | 0.3467 |
| 0.01 | 18.162 | 0.1816 | 0.6 | 0.596 | 3.0771 | 2.0975 | 0.100 | 64 | 0.1813 |
| 0 | 18.398 | 0 | 0.6 | 0.596 | $\infty$ | $\infty$ | 0.071 | 22 | 0 |
| 0.075 | 11.018 | 0.8264 | 0.6 | 0.596 | 0.3166 | 0.3124 | 3.368 | 2647 | 0.7010 |
| 0.075 | 11.018 | 0.8264 | 0.65 | 0.645 | 0.3166 | 0.3124 | 3.383 | 2849 | 0.7002 |
| 0.075 | 11.018 | 0.8264 | 0.7 | 0.694 | 0.3166 | 0.3124 | 3.368 | 3019 | 0.6990 |
| 0.075 | 11.018 | 0.8264 | 0.75 | 0.742 | 0.3166 | 0.3124 | 3.386 | 3166 | 0.6969 |
| 0.075 | 11.018 | 0.8264 | 0.8 | 0.789 | 0.3166 | 0.3124 | 3.330 | 3479 | 0.6976 |
| 0.075 | 11.018 | 0.8264 | 0.85 | 0.834 | 0.3166 | 0.3124 | 3.233 | 3583 | 0.6960 |
| 0.075 | 11.018 | 0.8264 | 0.9 | 0.876 | 0.3166 | 0.3124 | 3.167 | 3776 | 0.6950 |

[52–54] using the method of lines with fourth-order Runge-Kutta differencing in time and sixth-order stencils in space for improved phase accuracy [55]. The wide range of length scales is accommodated through adaptive mesh refinement provided by CARPET [56,57], and we compute apparent horizons with AHFINDERDIRECT [58,59]. We start our simulations with puncture [60] data of Bowen-York [61] type computed with Ansorg's spectral solver [62] inside the CACTUS TWOPUNCTURE thorn and evolve these using the moving puncture approach [63,64]. The gravitational wave signal is extracted in the form of the Newman-Penrose scalar $\Psi_4$ computed from the grid variables [49].

### B. Black-hole binary configurations

In this study, we consider equal-mass BH binaries in the superkick configuration; i.e., the BHs have spins of equal magnitude pointing in opposite directions in the orbital plane.[2] In practice, we do not compute the dimensionless spins $\chi_i$ directly from the Bowen-York spin, because some angular momentum and energy are contained in the spurious radiation of the conformally flat initial data. This energy and momentum are partly accreted onto the BHs and partly radiated to infinity, leading to a brief period of spin adjustment. While negligible for slowly rotating BHs, this effect increases for larger spin parameters and ultimately leads to a saturation at $\chi\sim 0.928$ [65,66]. In order to obtain a more accurate estimate of $\chi_i$, we monitor the BH spins $\boldsymbol{S}_i$ using the method described in Ref. [67] and compute the irreducible mass $m_{\mathrm{ir}}$ from the apparent horizon during the evolution. The dimensionless spin $\chi_i$ can then be computed according to [68]

$$M_i^2 = m_{\mathrm{ir},i}^2 + \frac{|\boldsymbol{S}_i|^2}{4m_{\mathrm{ir},i}^2}. \qquad \chi_i = \frac{|\boldsymbol{S}_i|}{M_i^2}. \tag{1}$$

As expected from the above description, we observe a brief transient period in all simulations during which $\chi_i$ mildly decreases. Throughout this work, we report the initial spin as the value at time $t_\chi = 20M$ measured from the beginning of the simulation. By this time, $\chi_i$ has reached a nearly stationary value, so that the precise value of $t_\chi$ does not affect the results. We distinguish this estimate for the initial spin from the value directly obtained from the Bowen-York parameters, which we denote by $\chi_{\mathrm{BY},i}$. The relation between $\chi_i$ and $\chi_{\mathrm{BY},i}$ is shown in the fourth and fifth columns of Table I. All simulations presented in this paper have $\chi_1=\chi_2$.

[2]We define here the orbital plane as the plane spanned by the initial position vector connecting the BHs and their initial linear momentum—in our case, this is the $xy$ plane, and the $z$ axis points in the direction perpendicular to this plane.

The net spin is zero in the superkick configurations, resulting in dynamics rather similar to those of nonspinning BH binaries; the main difference is a periodic motion of the orbital plane in the orthogonal (in our case $z$) direction. This motion of the binary orthogonal to the orbital plane results in a periodic blue- and redshift of the gravitational radiation, and the net effect of this beaming leads to asymmetric GW emission, especially in the $(\ell, m) = (2, 2)$ and $(2, -2)$ multipoles and, hence, net emission of linear momentum and the ensuing recoil of the postmerger remnant [14,15]. For fixed initial position $(\pm x_0, 0, 0)$ of the BH binary, the periodic nature of the blue- and redshifting of the gravitational radiation furthermore manifests itself in a sinusoidal dependence of the actual kick magnitude on the initial orientation of the spins in the orbital plane [14,69]. We quantify this orientation in terms of the angle $\alpha$ between the initial spin of the BH starting at $x > 0$ and the $x$ axis; i.e., this BH has initial spin $\boldsymbol{S}_1 = S(\cos\alpha, \sin\alpha, 0)$, while the BH at $x < 0$ is initialized with $\boldsymbol{S}_2 = -\boldsymbol{S}_1$ [14,23].

In order to assess the impact of the orbital eccentricity on the magnitude of the gravitational recoil, we have constructed a set of binary configurations guided by the second sequence of equal-mass, nonspinning BH binaries in Table I of Ref. [47]. This sequence starts with a quasicircular binary with initial separation $D/M = 7$ and a tangential linear momentum $p/M = 0.1247$ for each BH, resulting in an orbital angular momentum $L/M^2 = 0.8729$. These parameters determine the binding energy of the binary through $E_b \equiv M_{\rm ADM} - M$, where $M_{\rm ADM}$ is the Arnowitt-Deser-Misner (ADM) mass [70] of the binary spacetime. We construct a sequence of configurations with increasing eccentricity by gradually reducing the initial linear momentum parameter while keeping the binding energy fixed at $E_b/M = -0.012$. For this choice, the gradual reduction of initial kinetic energy for larger eccentricity implies a larger initial separation, i.e., correspondingly less negative potential energy, and, thus, ensures an inspiral phase of comparable duration irrespective of the eccentricity.

The variation in the initial separation of the BHs requires a minor change in the setup of the computational grid for low- and high-eccentricity binaries. In the notation of Ref. [49], we employ a grid setup given in units of $M$ by

$$\{(256, 128, 64, 32, 16, 8) \times (2, 1), h\},$$
$$\{(256, 128, 64, 32, 16) \times (4, 2, 1), h\}, \quad (2)$$

respectively, for binaries with $p/M \geq 0.8$ and those with $p/M < 0.8$. Here, the first line specifies a computational domain with six fixed outer grid components of cubic shape centered on the origin with radii 256, 128, 64, 32, 16, and 8, respectively, and two refinement levels with two cubic components each with radius 2 and 1 centered around either hole. The grid spacing is $h$ on the innermost level and successively increases by a factor of 2 on each next outer level. The second line in (2) likewise specifies a grid with five fixed and three dynamic refinement levels. Unless stated otherwise, we use a resolution $h = M/64$.

In order to accommodate the above-mentioned sinusoidal variation of the kick velocity with the initial spin orientation $\alpha$, we have performed for each value of the linear momentum parameter $p$ a subset of 6 runs with $\alpha \in [0, 180°)$. Due to the symmetry of the superkick configuration under a shift of the azimuthal angle $\phi \to \phi + 180°$, the recoil will always point in the $z$ direction with $v_x = v_y = 0$ [42,43]. Furthermore, two binaries with initial spin orientations $\alpha$ and $\alpha + 180°$ will generate kicks of equal magnitude but opposite direction, i.e., $v_z(\alpha) = -v_z(\alpha + 180°)$ [14]. Kick velocities for $\alpha \geq 180°$ can therefore be directly inferred through this symmetry from the simulations performed. For a few selected cases, we have performed additional simulations with $\alpha \geq 180°$; the symmetry is confirmed with accuracy of $\mathcal{O}(0.1)\%$ or better.

### C. Measuring the eccentricity

Our sequence of simulations is characterized by the variation of the orbital angular momentum at fixed binding energy. As discussed in detail in Ref. [47], there is no unambiguous way to assign an eccentricity parameter to BH binaries in the late stages of the inspiral. Motivated by the close similarity of the orbital dynamics of (equal-mass) superkick binaries and nonspinning binaries, we follow here the procedure used in Ref. [47] to obtain a PN estimate for nonspinning binaries. Specifically, we use Eqs. (20) and (25) of Ref. [48], which provide the PN eccentricity parameter $e_t$ for nonspinning binaries. This estimate needs to be taken with a grain of salt as it is only an approximation at the small binary separation during the last orbits before merger, and it ignores the effect of BH spins. Furthermore, $e_t$ exhibits an infinite gradient near the quasicircular limit when plotted as a function of the orbital angular momentum, leading to limited precision for values $e_t \lesssim 0.1$. Similarly, in the head-on limit, the vanishing of $L$ leads to a formal divergence of the eccentricity parameter, and a Newtonian interpretation ceases to be valid (values $e_t > 1$ are possible in this regime). Nevertheless, $e_t$ provides us with a rough estimate to quantify deviations from the quasicircular case and distinguish low-, moderate-, and high-eccentricity configurations.

For all simulations, we have computed the following diagnostic variables. The energy, linear, and angular momentum radiated in GWs are computed on extraction spheres of coordinate radius $r_{\rm ex}/M = 30, 40, \ldots, 90$ from the Newman-Penrose scalar according to the standard methods described, for example, in Ref. [71]. For the physical radiation reported in Table I, we exclude the spurious radiation inherent in the initial data by considering only the wave signal starting at retarded time $u \equiv t - r_{\rm ex} = 50M$. We also compute the dimensionless spin of the postmerger BH from the apparent

horizon [72]. We have confirmed these values using also the conservation of energy and angular momentum, which yields agreement to within 0.5% or better.

### D. Numerical accuracy

Our numerical results for the GW emission and the recoil velocities are affected by two main sources of uncertainty: the discretization error and the finite extraction radii for the Newman-Penrose scalar.

We address the latter by extrapolating the GW signal to infinity using a Taylor series in $1/r$ as in Ref. [73]. The results reported are those extrapolated at linear order in $1/r$, and we estimate the error through the difference with respect to a second-order extrapolation. The magnitude of this error is approximately 2% or less.

In order to assess the error due to finite differencing, we have performed additional simulations of the configuration $p/M = 0.1247$, $\chi_i = 0.596$, $\alpha = 150°$ using grid resolutions $h = M/48$ and $h = M/80$. Figure 2 shows convergence between fourth and fifth order resulting in a discretization error of about 2% for the radiated linear momentum. A similar behavior is observed for the radiated energy $E_{\rm rad}$. We use this value as an error estimate, but note that this is a conservative estimate for the *maximum* kick velocity at fixed eccentricity. The reason is that a considerable part of the numerical error consists in the inaccuracy of the inspiral phase of the binary. This phase error significantly affects the angle $\alpha_0$ in Eq. (3) below, but has weaker repercussions on the maximum kick $v_{\rm max}$. In other words, at lower resolution, we will obtain the maximum kick at a "wrong" phase angle $\alpha_0$, but still measure this maximum with decent precision. We have verified this expectation by generating a complete sequence for $p/M = 0.1247$, $\chi_i = 0.596$ at low, medium, and high resolution. Applying the fit (3) to each of these gives us $v_{\rm max} = 2098.1$, 2108.3, and 2109.7 km/s, respectively, for $h/M = 1/48$, $1/64$, and $1/80$. Since we cannot entirely rule out fortuitous cancellation of errors in this excellent agreement, we keep in the remainder of this work the more conservative 2% estimate from Fig. 2. Combined with the extrapolation procedure to $r_{\rm ex} \to \infty$, we estimate our total error budget as approximately 4%.

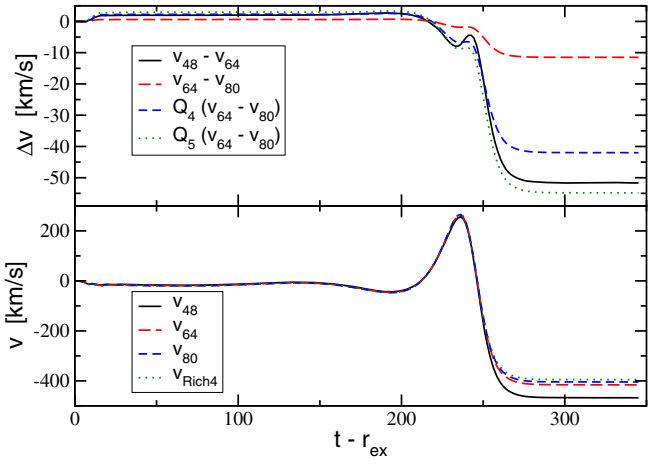


FIG. 2. Convergence analysis for the linear momentum radiated from a binary with $p/M = 0.1247$, $\chi_i = 0.596$, $\alpha = 150°$. The linear momentum obtained for resolutions $h = M/48$, $h = M/64$, and $h = M/80$ is shown in the form of the kick velocity accumulated up to retarded time $u = t - r_{\rm ex}$ in the bottom panel. The upper panel shows differences between various resolutions, together with rescaling according to fourth- and fifth-order convergence. We estimate the uncertainty from the more conservative fourth-order Richardson extrapolation, and we obtain a numerical error estimate of about 2% for our standard resolution $h = M/64$.

## III. NUMERICAL RESULTS

The main results of our study are summarized in Table I. For each sequence with prescribed linear momentum $p$, we list there the initial separation $D$, orbital angular momentum $L$, the initial BH spins $\chi_{{\rm BY},i}$ and $\chi_i$, eccentricity estimates $e_t$ obtained in ADMTT and harmonic gauge according to Eqs. (20) and (25) of Ref. [48], the mean radiated energy $E_0$, the maximum kick velocity $v_{\rm max}$, and the dimensionless spin $\chi_0$ of the merger remnant.

### A. Impact of the orbital eccentricity

The sinusoidal dependence of the kick magnitude on the initial spin orientation $\alpha$ is illustrated in Fig. 3 for the case $p/M = 0.075$, $\chi_i = 0.596$. The data are reproduced with high precision by a fit of the form

$$v_{\rm kick} = v_{\rm max} \times \cos(\alpha - \alpha_0), \tag{3}$$

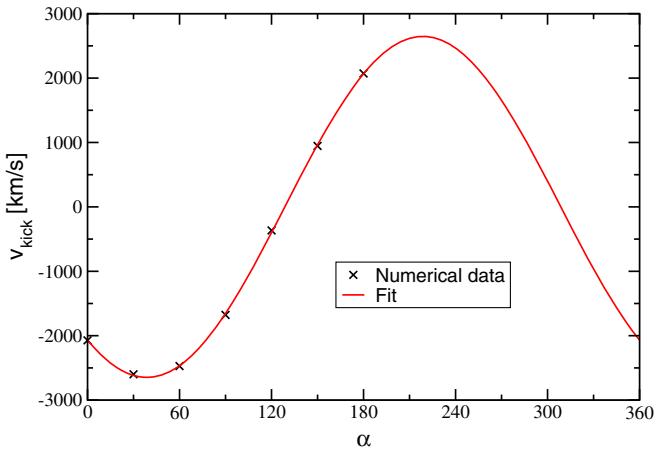


FIG. 3. The recoil velocity computed numerically from the GW signal for $p = 0.075$ is shown as $\times$ symbols for different values of the spin orientation $\alpha$. The red curve represents the fit obtained from these data according to Eq. (3). Only data for $\alpha < 180°$ are needed to determine the fitting coefficients, due to the symmetry of the superkick configurations.

where, for this specific series, $v_{\rm max} = 2647$ km/s and $\alpha_0 = 218.7°$. The radiated energy $E_{\rm rad}$ and the final spin, in contrast, vary only mildly (within the numerical uncertainties) with the angle $\alpha$; we report average values for these quantities. More specifically, we fit $E_{\rm rad} = E_0 + E_1 \sin(2\alpha + \alpha_0)$ and report $E_0$ (and likewise $\chi_0$).

The variation of the kick velocity with eccentricity is visualized in the left panel of Fig. 1, which shows $v_{\rm max}$ as a function of the linear momentum $p$. We clearly see that the largest kicks are not realized for quasicircular binaries but for moderate eccentricities. The similar effect is apparent for the radiated energy values of Table I, which closely resembles the observation in Table I of Ref. [47] for the nonspinning case. The increase in the recoil velocity, however, is much stronger: for $p/M = 0.75$, the maximum kick exceeds the quasicircular value by about 25%, while the largest energy represents a meager 5% increase relative to the quasicircular case. This discrepancy shows that the enhanced kick is not merely due to increased radiation but also to a higher degree of asymmetry in eccentric binaries.

An increase in the recoil at small eccentricities has already been noticed in the close-limit calculations of Refs. [44,74], which find a $(1 + e)$ proportionality for eccentricities $e \lesssim 0.1$. In the right panel of Fig. 1, we plot the maximum kick velocity as a function of the eccentricity parameter $e_t$ in harmonic gauge (the ADMTT version of $e_t$ would result in virtually the same figure). Due to the diverging gradient of $e_t$ with respect to the orbital angular momentum [47], our data points are limited to $e_t \gtrsim 0.1$, but as shown in the inset of the figure, the data are compatible with the linear growth $\propto (1 + e_t)$ of the close-limit approximation. The two fits shown in the inset have been obtained using either the first four or the first five data points with the expression $v_{\rm max} = v_0(1 + e_t)$. The numerical results suggest that above $e_t \approx 0.2$, $v_{\rm max}$ increases even more strongly with $e_t$ before reaching the maximum at $e_t \approx 0.3$, and then decreases for yet higher eccentricity.

### B. Impact of the spin magnitudes

The gravitational recoil in superkick configurations is known to increase approximately linearly with the spin magnitudes $\chi_i$. Extrapolating numerical results to maximal spin $\chi_i = 1$ results in a maximal superkick of about 3680 km/s [69] for quasicircular binaries. We will now investigate to what extent nonzero eccentricity can increase this upper limit. In order to keep the computational costs manageable, we focus for this purpose on the $p/M = 0.75$ sequence which maximizes the recoil in our eccentricity analysis for $\chi_i = 0.596$. We cannot rule out that the "optimal" eccentricity maximizing recoil depends on the spin magnitude, so our analysis should be regarded as a conservative estimate; the largest possible superkick in eccentric binaries may even exceed the value resulting from the analysis below.

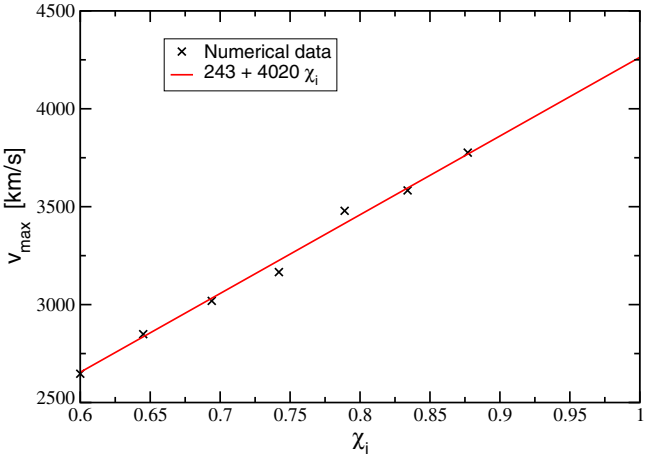


FIG. 4. The maximum recoil velocity $v_{\rm max}$ for $p/M = 0.075$ as a function of the initial spin magnitude $\chi_i$. The curve represents the linear fit (4).

We vary the initial spin magnitude $\chi_i$ while keeping all other parameters, including the eccentricity $e_t$, fixed. A convergence analysis for $\chi_i = 0.9$ yields a similar order as in Fig. 2, but demonstrates that higher resolution is needed for these configurations. We use $h = M/80$ for the simulations discussed in this subsection, which results in a discretization error of about 4%. As before, we cover the range of the initial spin orientation by evolving six binaries with $\alpha \in [0, 180°)$ for each value of $\chi_i$ and fit the resulting $v_{\rm kick}$ according to the sinusoidal function of Eq. (3). The results for these simulations are listed in the lower block of Table I. As expected, the maximum recoil velocity $v_{\rm max}$ increases with the spins $\chi_i$. We display $v_{\rm max}$ as a function of $\chi_i$ in Fig. 4, together with a linear fit to model the leading-order dependence of the maximum recoil velocity $v_{\rm max}$ on the spin magnitude $\chi_i$ [8,69]. This fit is given by

$$v_{\rm max} = [(243 \pm 122) + (4020 \pm 163)\chi_i] \text{ km/s} \quad (4)$$

and predicts a maximum kick of $4263 \pm 285$ km/s for extremal spins $\chi_i = 1$. This value exceeds the maximal superkick for quasicircular binaries of about 3680 km/s [8,69] by about 16%, but falls short of the 5000 km/s maximum for the hang-up kicks reported in Ref. [10]. To the best of our knowledge, the effect of eccentricity on these hang-up kicks has not yet been explored. The results reported here and the findings of Ref. [44] hint that yet larger recoils may be possible in bound BH binary systems.

## IV. CONCLUSIONS

Orbital eccentricity amplifies superkicks. We have presented an extensive series of numerical simulations of merging BHs with spin vectors of magnitude approximately 0.6 in the orbital plane and initially antialigned with each other. We then vary the initial linear momentum of the holes for fixed binding energy, which is equivalent to

modifying the initial eccentricity. We find that orbital eccentricity can boost the final recoil by up to approximately 25%. The binaries that receive the largest kick of approximately 2600 km/s have moderate eccentricity $e_t \sim 0.3$ [47,48]. For comparison, the maximal kick imparted to a quasicircular binary with the same parameters is approximately 2100 km/s. Our results suggest that the enhanced radiation of linear momentum is mainly due to the more pronounced asymmetry in the binary's GW emission rather than the mere consequence of a larger energy flux.

An additional series of simulations with fixed eccentricity and varying spin magnitudes allows us to extrapolate these results to maximally rotating BHs. We predict a maximum superkick of at least approximately 4300 km/s, compared to the quasicircular result of approximately 3700 km/s. We stress that this estimate is conservative because i) we did not explore the optimal value of the eccentricity as a function of the spin magnitude and ii) we constrained the spins to the orbital plane; partial alignment is known to generate larger recoils [10,11]. The impact of orbital eccentricity on these *hang-up* kicks with partial spin alignment is a complex task that we leave for future work: the recoil has a more complicated dependence on the eccentricity and the initial spin orientations because of spin precession.

The amplification of superkicks due to orbital eccentricity may have important consequences for the modeling of GW sources. For the stellar-mass BHs targeted by ground-based interferometers, a non-negligible eccentricity at merger would be a powerful signature of strong and recent interactions with external bodies (cf. e.g., Refs. [75,76,76–81]). If BH binaries coalescing in dynamical environments are indeed eccentric, our findings further limit the ability of a stellar cluster to retain their merger remnants [32]. For instance, Refs. [82,83] found that dynamical interactions in globular clusters are a viable formation mechanism to explain multiple generations of eccentric BH mergers. The calculation of the retention fraction, however, does not take into account the significant kick enhancement due to eccentricity that we have found in this work. Given the low escape speed of globular clusters, this amplification may considerably reduce the predicted number of second-generation BH mergers.

For the case of supermassive BH binaries, eccentric sources are commonly invoked to explain current PTA limits. Orbital eccentricity shifts some of the emitted power to higher frequencies, causing a turnover in the predicted spectrum [84–87]. The presence of this feature allows current astrophysical formation models calibrated on galaxy counts to more easily accommodate the measured upper limits. Our work highlights that kicks may be higher than currently assumed, further reducing the merger rate and the predicted stochastic GW background.

Numerical-relativity simulations now provide a thorough understanding of the properties of the BH remnants left behind following mergers of BHs on quasicircular orbits. Efficient and accurate models for final mass, spin, and kick are available and routinely implemented in astrophysical predictions. For eccentric orbits, the additional dimensionality of the parameter space increases the computational resources required to accurately predict waveforms and remnant properties. Comparatively few numerical studies have focused on the eccentric regime in the past [47,88,89], but more recently, systematic efforts in GW modeling have expanded into the eccentric regime [90]. We hope that our findings have further demonstrated the fertile ground of this class of binaries and that they will spark future work in this direction.

## ACKNOWLEDGMENTS

We thank V. Baibhav for discussions. U.S. is supported by the European Union's H2020 ERC Consolidator Grant "Matter and strong-field gravity: new frontiers in Einstein's theory" Grant No. MaGRaTh–646597 and the STFC Consolidator Grant No. ST/P000673/1. D. G. is supported by Leverhulme Trust Grant No. RPG-2019-350. E. B. is supported by NSF Grant No. PHY-1912550, NSF Grant No. AST-1841358, NASA ATP Grant No. 17-ATP17-0225, and NASA ATP Grant No. 19-ATP19-0051. This work has received funding from the European Union's Horizon 2020 research and innovation programme under the Marie Skłodowska-Curie Grant No. 690904. This work was supported by the GWverse COST Action Grant No. CA16104, "Black holes, gravitational waves and fundamental physics." Computational work was performed on the SDSC Comet and TACC Stampede2 clusters through NSF-XSEDE Grant No. PHY-090003, Cambridge CSD3 system through STFC capital Grants No. ST/P002307/1 and No. ST/R002452/1, and STFC operations Grant No. ST/R00689X/1; the University of Birmingham BlueBEAR cluster; the Athena cluster at HPC Midlands +funded by EPSRC Grant No. EP/P020232/1; and the Maryland Advanced Research Computing Center.

[1] W. B. Bonnor and M. A. Rotenberg, Proc. R. Soc. A **265**, 109 (1961).
[2] A. Peres, Phys. Rev. **128**, 2471 (1962).
[3] J. D. Bekenstein, Astrophys. J. **183**, 657 (1973).
[4] M. J. Fitchett, Mon. Not. R. Astron. Soc. **203**, 1049 (1983).
[5] M. Favata, S. A. Hughes, and D. E. Holz, Astrophys. J. **607**, L5 (2004).
[6] L. Blanchet, M. S. S. Qusailah, and C. M. Will, Astrophys. J. **635**, 508 (2005).
[7] J. A. González, M. Hannam, U. Sperhake, B. Brügmann, and S. Husa, Phys. Rev. Lett. **98**, 231101 (2007).
[8] M. Campanelli, C. O. Lousto, Y. Zlochower, and D. Merritt, Phys. Rev. Lett. **98**, 231102 (2007).
[9] W. Tichy and P. Marronetti, Phys. Rev. D **76**, 061502(R) (2007).
[10] C. O. Lousto and Y. Zlochower, Phys. Rev. Lett. **107**, 231102 (2011).
[11] C. O. Lousto and Y. Zlochower, Phys. Rev. D **87**, 084027 (2013).
[12] Y. Zlochower and C. O. Lousto, Phys. Rev. D **92**, 024022 (2015); **94**, 029901(E) (2016).
[13] C. O. Lousto and J. Healy, Phys. Rev. D **100**, 104039 (2019).
[14] B. Brügmann, J. A. González, M. Hannam, S. Husa, and U. Sperhake, Phys. Rev. D **77**, 124047 (2008).
[15] F. Pretorius, in *Physics of Relativistic Objects in Compact Binaries: From Birth to Coalescence*, edited by M. Colpi *et al.* (Springer, New York, 2009).
[16] J. D. Schnittman, A. Buonanno, J. R. van Meter, J. G. Baker, W. D. Boggs, J. Centrella, B. J. Kelly, and S. T. McWilliams, Phys. Rev. D **77**, 044031 (2008).
[17] D. Gerosa and C. J. Moore, Phys. Rev. Lett. **117**, 011101 (2016).
[18] J. Calderón Bustillo, J. A. Clark, P. Laguna, and D. Shoemaker, Phys. Rev. Lett. **121**, 191102 (2018).
[19] J. Healy, F. Herrmann, I. Hinder, D. M. Shoemaker, P. Laguna, and R. A. Matzner, Phys. Rev. Lett. **102**, 041101 (2009).
[20] U. Sperhake, E. Berti, V. Cardoso, F. Pretorius, and N. Yunes, Phys. Rev. D **83**, 024037 (2011).
[21] J. Centrella, J. G. Baker, B. J. Kelly, and J. R. van Meter, Rev. Mod. Phys. **82**, 3069 (2010).
[22] U. Sperhake, in *Gravitational Wave Astrophysics*, Astrophysics and Space Science Proceedings, edited by C. F. Sopuerta (Springer International Publishing Switzerland, Switzerland, 2015), Vol. 40, pp. 185–202, https://doi.org/10.1007/978-3-319-10488-1_16.
[23] D. Gerosa, F. Hébert, and L. C. Stein, Phys. Rev. D **97**, 104049 (2018).
[24] D. Merritt, M. Milosavljević, M. Favata, S. A. Hughes, and D. E. Holz, Astrophys. J. **607**, L9 (2004).
[25] M. J. Benacquista and J. M. B. Downing, Living Rev. Relativity **16**, 4 (2013).
[26] J. A. González, U. Sperhake, B. Brügmann, M. Hannam, and S. Husa, Phys. Rev. Lett. **98**, 091101 (2007).
[27] J. Morawski, M. Giersz, A. Askar, and K. Belczynski, Mon. Not. R. Astron. Soc. **481**, 2168 (2018).
[28] K. Holley-Bockelmann, K. Gültekin, D. Shoemaker, and N. Yunes, Astrophys. J. **686**, 829 (2008).
[29] F. Antonini and F. A. Rasio, Astrophys. J. **831**, 187 (2016).
[30] N. C. Stone, B. D. Metzger, and Z. Haiman, Mon. Not. R. Astron. Soc. **464**, 946 (2017).
[31] I. Bartos, B. Kocsis, Z. Haiman, and S. Márka, Astrophys. J. **835**, 165 (2017).
[32] D. Gerosa and E. Berti, Phys. Rev. D **100**, 041301(R) (2019).
[33] D. Gerosa and A. Sesana, Mon. Not. R. Astron. Soc. **446**, 38 (2015).
[34] L. Blecha and A. Loeb, Mon. Not. R. Astron. Soc. **390**, 1311 (2008).
[35] A. Sesana, Mon. Not. R. Astron. Soc. **382**, L6 (2007).
[36] T. Bogdanović, C. S. Reynolds, and M. C. Miller, Astrophys. J. **661**, L147 (2007).
[37] G. Lodato and D. Gerosa, Mon. Not. R. Astron. Soc. **429**, L30 (2013).
[38] M. C. Miller and J. H. Krolik, Astrophys. J. **774**, 43 (2013).
[39] D. Gerosa, B. Veronesi, G. Lodato, and G. Rosotti, Mon. Not. R. Astron. Soc. **451**, 3941 (2015).
[40] M. Kesden, U. Sperhake, and E. Berti, Astrophys. J. **715**, 1006 (2010).
[41] E. Berti, M. Kesden, and U. Sperhake, Phys. Rev. D **85**, 124049 (2012).
[42] L. Boyle, M. Kesden, and S. Nissanke, Phys. Rev. Lett. **100**, 151101 (2008).
[43] L. Boyle and M. Kesden, Phys. Rev. D **78**, 024017 (2008).
[44] C. F. Sopuerta, N. Yunes, and P. Laguna, Astrophys. J. **656**, L9 (2007).
[45] L. E. Kidder, Phys. Rev. D **52**, 821 (1995).
[46] M. Campanelli, C. O. Lousto, Y. Zlochower, and D. Merritt, Phys. Rev. Lett. **98**, 231102 (2007).
[47] U. Sperhake, E. Berti, V. Cardoso, J. A. González, B. Brügmann, and M. Ansorg, Phys. Rev. D **78**, 064069 (2008).
[48] R.-M. Memmesheimer, A. Gopakumar, and G. Schäfer, Phys. Rev. D **70**, 104011 (2004).
[49] U. Sperhake, Phys. Rev. D **76**, 104015 (2007).
[50] G. Allen, T. Goodale, J. Massó, and E. Seidel, in *Proceedings of Eighth IEEE International Symposium on High Performance Distributed Computing* (IEEE, New York, 1999).
[51] Cactus Computational Toolkit homepage, www.cactuscode.org.
[52] T. Nakamura, K. Oohara, and Y. Kojima, Prog. Theor. Phys. Suppl. **90**, 1 (1987).
[53] M. Shibata and T. Nakamura, Phys. Rev. D **52**, 5428 (1995).
[54] T. W. Baumgarte and S. L. Shapiro, Phys. Rev. D **59**, 024007 (1998).
[55] S. Husa, J. A. González, M. Hannam, B. Brügmann, and U. Sperhake, Classical Quantum Gravity **25**, 105006 (2008).
[56] E. Schnetter, S. H. Hawley, and I. Hawke, Classical Quantum Gravity **21**, 1465 (2004).
[57] Carpet Code homepage, www.carpetcode.org.
[58] J. Thornburg, Phys. Rev. D **54**, 4899 (1996).
[59] J. Thornburg, Classical Quantum Gravity **21**, 743 (2004).
[60] S. Brandt and B. Brügmann, Phys. Rev. Lett. **78**, 3606 (1997).
[61] J. M. Bowen and J. W. York, Jr, Phys. Rev. D **21**, 2047 (1980).
[62] M. Ansorg, B. Brügmann, and W. Tichy, Phys. Rev. D **70**, 064011 (2004).

[63] J. G. Baker, J. Centrella, D.-I. Choi, M. Koppitz, and J. van Meter, Phys. Rev. Lett. **96**, 111102 (2006).
[64] M. Campanelli, C. O. Lousto, P. Marronetti, and Y. Zlochower, Phys. Rev. Lett. **96**, 111101 (2006).
[65] G. B. Cook and J. W. York, Jr, Phys. Rev. D **41**, 1077 (1990).
[66] S. Dain, C. O. Lousto, and R. Takahashi, Phys. Rev. D **65**, 104038 (2002).
[67] M. Campanelli, C. O. Lousto, Y. Zlochower, B. Krishnan, and D. Merritt, Phys. Rev. D **75**, 064030 (2007).
[68] D. Christodoulou, Phys. Rev. Lett. **25**, 1596 (1970).
[69] M. Campanelli, C. Lousto, Y. Zlochower, and D. Merritt, Astrophys. J. **659**, L5 (2007).
[70] R. Arnowitt, S. Deser, and C. W. Misner, in *Gravitation an Introduction to Current Research*, edited by L. Witten (Wiley, New York, 1962), pp. 227–265.
[71] M. Ruiz, M. Alcubierre, D. Núñez, and R. Takahashi, Gen. Relativ. Gravit. **40**, 1705 (2008).
[72] W. G. Cook, D. Wang, and U. Sperhake, Classical Quantum Gravity **35**, 235008 (2018).
[73] U. Sperhake, B. Brügmann, D. Müller, and C. F. Sopuerta, Classical Quantum Gravity **28**, 134004 (2011).
[74] C. F. Sopuerta, N. Yunes, and P. Laguna, Phys. Rev. D **74**, 124010 (2006); **78**, 049901(E) (2008).
[75] F. Antonini and H. B. Perets, Astrophys. J. **757**, 27 (2012).
[76] J. Samsing, Phys. Rev. D **97**, 103014 (2018).
[77] L. Gondán, B. Kocsis, P. Raffai, and Z. Frei, Astrophys. J. **860**, 5 (2018).
[78] J. Samsing, A. Askar, and M. Giersz, Astrophys. J. **855**, 124 (2018).
[79] M. Zevin, J. Samsing, C. Rodriguez, C.-J. Haster, and E. Ramirez-Ruiz, Astrophys. J. **871**, 91 (2019).
[80] G. Fragione and A. Loeb, Mon. Not. R. Astron. Soc. **486**, 4443 (2019).
[81] J. Samsing, D. J. D'Orazio, K. Kremer, C. L. Rodriguez, and A. Askar, arXiv:1907.11231.
[82] C. L. Rodriguez, P. Amaro-Seoane, S. Chatterjee, and F. A. Rasio, Phys. Rev. Lett. **120**, 151101 (2018).
[83] C. L. Rodriguez, M. Zevin, P. Amaro-Seoane, S. Chatterjee, K. Kremer, F. A. Rasio, and C. S. Ye, Phys. Rev. D **100**, 043027 (2019).
[84] M. Enoki and M. Nagashima, Prog. Theor. Phys. **117**, 241 (2007).
[85] A. Sesana, Astrophys. J. **719**, 851 (2010).
[86] E. A. Huerta, S. T. McWilliams, J. R. Gair, and S. R. Taylor, Phys. Rev. D **92**, 063010 (2015).
[87] S. R. Taylor, E. A. Huerta, J. R. Gair, and S. T. McWilliams, Astrophys. J. **817**, 70 (2016).
[88] I. Hinder, B. Vaishnav, F. Herrmann, D. M. Shoemaker, and P. Laguna, Phys. Rev. D **77**, 081502(R) (2008).
[89] I. Hinder, F. Herrmann, P. Laguna, and D. Shoemaker, Phys. Rev. D **82**, 024033 (2010).
[90] A. Ramos-Buades, S. Husa, G. Pratten, H. Estellés, C. García-Quirós, M. Mateu, M. Colleoni, and R. Jaume, arXiv:1909.11011.